

PLANETS AROUND LOW-MASS STARS (PALMS).  
II. A LOW-MASS COMPANION TO THE YOUNG M DWARF GJ 3629 SEPARATED BY 0<sup>0</sup>.2\*

BRENDAN P. BOWLER,<sup>1</sup> MICHAEL C. LIU,<sup>1</sup> EVGENYA L. SHKOLNIK,<sup>2</sup> AND MOTOHIDE TAMURA<sup>3</sup>  
*ApJ, in press*

ABSTRACT

We present the discovery of a 0<sup>0</sup>.2 companion to the young M dwarf GJ 3629 as part of our high contrast adaptive optics imaging search for giant planets around low-mass stars with the Keck-II and Subaru telescopes. Two epochs of imaging confirm the pair is co-moving and reveal signs of orbital motion. The primary exhibits saturated X-ray emission, which together with its UV photometry from *GALEX* point to an age younger than  $\sim 300$  Myr. At these ages the companion lies below the hydrogen burning limit with a model-dependent mass of  $46 \pm 16 M_{\text{Jup}}$  based on the system's photometric distance of  $22 \pm 3$  pc. Resolved *YJHK* photometry of the pair indicates a spectral type of  $M7 \pm 2$  for GJ 3629 B. With a projected separation of  $4.4 \pm 0.6$  AU and an estimated orbital period of  $21 \pm 5$  yr, GJ 3629 AB is likely to yield a dynamical mass in the next several years, making it one of only a handful of brown dwarfs to have a measured mass and an age constrained from the stellar primary.

*Subject headings:* stars: individual (GJ 3629) — stars: low-mass, brown dwarfs

1. INTRODUCTION

Following a decade of attempts to directly image extrasolar giant planets with increasingly sensitive instruments and speckle suppression techniques (e.g., Lowrance et al. 2005; Biller et al. 2007; Lafrenière et al. 2007; Liu et al. 2010b), several planetary systems have finally been found through high contrast imaging over the past few years. These discoveries have opened up an exciting new era of planetary science where the atmospheres of non-transiting extrasolar planets can be directly studied for the first time. Five unambiguous planets have been imaged orbiting two stars: one around the A5 star  $\beta$  Pic (Lagrange et al. 2009; Lagrange et al. 2010), and four surrounding the A5 star HR 8799 (Marois et al. 2008; Marois et al. 2010).<sup>5</sup> The

fact that all these planets orbit high-mass stars might at first suggest that giant planet formation is more efficient around massive stars, which is a well-established trend observed at smaller separations from radial velocity planet searches (Johnson et al. 2007; Lovis & Mayor 2007; Bowler et al. 2010; Johnson et al. 2010). However, high contrast imaging searches have mostly neglected low-mass stars. Until recently there has been a scarcity of known nearby young M dwarfs, making it difficult to produce statistical comparisons of planet occurrence rates as a function of stellar mass. As a result, even though M dwarfs outnumber AFGK stars by a factor of 2–3 in the solar neighborhood (Henry et al. 1997; Bochanski et al. 2010), our understanding of planet formation is the weakest in this stellar mass regime.

We are conducting a high contrast adaptive optics imaging survey of young M dwarfs with Keck-II and Subaru to search for young giant planets and brown dwarfs and measure the frequency of giant planets orbiting low-mass stars. Our targets are newly identified M dwarfs with ages  $< 300$  Myr and distances  $\lesssim 30$  pc which were selected based on elevated levels of X-ray and UV emission (Shkolnik et al. 2009; Shkolnik et al. 2011). Compared to high-mass stars, M dwarfs present several advantages as targets for direct imaging. Their higher space densities mean they are on average closer than more massive stars, so smaller physical separations can be probed. Moreover, because M dwarfs are intrinsically faint, direct imaging can detect lower planet masses in the contrast-limited regime. This allows us to reach typical planet masses of a few  $M_{\text{Jup}}$  at separations of  $\sim 10$  AU, making our Planets Around Low-Mass Stars (PALMS) survey one of the deepest direct imaging planet searches to date.

The first discovery from our PALMS survey was an L0 substellar companion to the young M dwarf 1RXS J235133.3+312720 separated by  $\sim 120$  AU (Bowler et al. 2012). Here we present the discovery of a 0<sup>0</sup>.2 companion to the young M3.0 star GJ 3629. Shkolnik et al. (2009) identified GJ 3629 as a young star

bbowler@ifa.hawaii.edu

<sup>1</sup> Institute for Astronomy, University of Hawai'i, 2680 Woodlawn Drive, Honolulu, HI 96822, USA

<sup>2</sup> Lowell Observatory, 1400 W. Mars Hill Road, Flagstaff, AZ 86001

<sup>3</sup> National Astronomical Observatory of Japan, 2-21-1 Osawa, Mitaka, Tokyo 181-8588, Japan

\* Some of the data presented herein were obtained at the W.M. Keck Observatory, which is operated as a scientific partnership among the California Institute of Technology, the University of California and the National Aeronautics and Space Administration. The Observatory was made possible by the generous financial support of the W.M. Keck Foundation.

<sup>5</sup> Because the optically-detected companion to Fomalhaut (Kalas et al. 2008) has not been recovered in the infrared (Marengo et al. 2009), it is unclear whether the object is a planet, perhaps with a large high-albedo ring system, or something else, like a dust cloud from a recent planetesimal collision (Janson et al. 2012). Recently Kraus & Ireland (2012) have discovered what appears to be a young ( $\sim 2$  Myr) accreting giant planet orbiting the transition-disk star LkCa 15 at  $\sim 15$ – $20$  AU, but a clear understanding of this system, including the mass of the companion, is still lacking. In addition to these objects, a handful of other planetary-mass companions have been found orbiting stars from hundreds (e.g., 1RXS J1609–2105 b: Lafrenière et al. 2008; GSC 06214–00210 b: Ireland et al. 2011) to thousands (Ross 458 C: Goldman et al. 2010, Scholz 2010; WD 0806-661 B: Luhman et al. 2011) of AU, but the formation mechanism of these enigmatic companions remains obscure (e.g., Bowler et al. 2011).

based on its high fractional X-ray luminosity, which is comparable to members of the Pleiades ( $\sim 125$  Myr) and young moving groups (10–100 Myr). Shkolnik et al. (2009) obtained a high resolution optical spectrum of GJ 3629 A and did not detect Li, thereby setting a lower limit to its age. Based on these constraints they estimate an age of 25–300 Myr, which places our new companion GJ 3629 B below the hydrogen burning minimum mass at the estimated distance of the system ( $22 \pm 3$  pc; Section 3.1).

## 2. KECK-2/NIRC2 NGS AO IMAGING

We imaged GJ 3629 on 25 March 2011 UT with the Near Infrared Camera 2 (NIRC2) in its narrow-field mode on Keck-II coupled with natural guide star adaptive optics (NGS AO; Wizinowich et al. 2000). There were light cirrus clouds during the observations and the seeing was  $\sim 0''.6$  as reported by the Differential Imaging Motion Monitor on CFHT. We obtained three short dithered frames with the  $K_S$  filter while reading out the central  $512 \times 512$  pixels. GJ 3629 was easily resolved into a  $\sim 200$  mas pair with a flux ratio of  $\sim 3$  mag (the diffraction limit in  $K$  is  $\sim 55$  mas). Second-epoch observations were obtained on 3 March 2012 UT with Keck-II/NIRC2 (narrow-field) and NGS AO. Humidity levels were near 100% most of night and there were several bouts of snow, but for about half an hour the humidity dropped and the sky was clear enough to observe GJ 3629 in order to verify the companion was comoving with the primary. We imaged the system in dithered patterns with the  $YJHK$  filters (Figure 1), which are from the Mauna Kea Observatory filter system (Simons & Tokunaga 2002; Tokunaga & Vacca 2005). A summary of our observations are listed in Table 1.

The images were reduced in the standard fashion by removing bad pixels, subtracting dark frames, and dividing by normalized dome flats obtained at the start of the night. Each image was North-aligned using the FITS header keywords, taking into account the AO-detector offset ( $+0.7^\circ$ ) and the sky orientation on the detector ( $+0.252^\circ$ ) derived by Yelda et al. (2010). We computed astrometry and flux ratios by fitting an analytic model composed of three elliptical Gaussians to each binary component as described in Liu et al. (2008). We found that varying the number of Gaussians in the input PSF model (two versus three) resulted in systematic errors in the flux ratios of  $\approx 1\%$ , so we incorporated this in our flux ratio uncertainty by adding it in quadrature with the measured random errors. No distortion correction was applied because the relative correction over  $\sim 20$  pixels is negligible for our purposes. For the separation measurement we adopt the NIRC2 plate scale of  $9.952 \pm 0.002$  mas  $\text{pix}^{-1}$  derived by Yelda et al. (2010). The resulting astrometry and flux ratios are listed in Table 2, where the quoted values and uncertainties represent the means and standard deviations of each data set. Strehl ratios and full width at half-maximum (FWHM) measurements of GJ 3629 A were made with the publicly available IDL routine NIRC2STREHL and are listed alongside the astrometry in Table 2.

## 3. RESULTS

### 3.1. Distance

There is no parallax measurement for GJ 3629 A but there are several distance estimates to the primary in the literature. GJ 3629 is part of the *NStars* sample of nearby stars ( $\lesssim 20$  pc; Reid et al. 1995; Reid et al. 2004) and was assigned a spectrophotometric distance of  $16.7 \pm 2.7$  pc (Shkolnik et al. 2009) based on optical bandstrength-absolute magnitude relations. Recently Shkolnik et al. (2012, submitted) measured parallaxes for 75 young ( $< 300$  Myr) M-type stars with spectrophotometric distance estimates  $< 30$  pc. They found that the photometric distances were typically underestimated by  $\sim 70\%$  as a result of unresolved binarity and youthful overluminosity, which would place GJ 3629 AB at  $\sim 28$  pc. Shkolnik et al. (2012, submitted) also derive a distance estimate using the minimum (25 Myr) and maximum (300 Myr) age estimates of the system (Section 3.3) combined with the evolutionary models of Baraffe et al. (1998), arriving at a value of  $22 \pm 7$  pc. Other independent distance estimates for the system include photometric distances of  $18^{+8}_{-4}$  pc and  $22.2 \pm 5.6$  pc by Lépine & Gaidos (2011) and Lépine & Shara (2005), which were computed using color-absolute magnitude relations from field M dwarfs, and an estimate of 26 pc by Wright et al. (2011) using 1 Gyr theoretical isochrones from Siess et al. (2000). Given this large range of distance estimates, we adopt a value of  $22 \pm 3$  pc for GJ 3629 AB.

### 3.2. Common Proper Motion

The baseline of 11 months between our first and second epoch observations lets us easily distinguish whether the close companion is physically bound to the primary. Figure 2 shows the expected relative motion of a stationary background object based on the proper and parallactic motion of GJ 3629. The gray 1- and 2- $\sigma$  confidence intervals for the background tracks in Figure 2 are based on Monte Carlo realizations incorporating uncertainties in the distance estimate, proper motion, and astrometry. The weighted mean of the second epoch astrometry from our four independent measurements (one for each filter) is  $197.9 \pm 0.2$  mas and  $120.75 \pm 0.07^\circ$ . If the candidate companion was a distant background object then the expected separation ( $352 \pm 3$  mas) and position angle ( $100.8 \pm 0.9^\circ$ ) at the time of our second epoch observation would differ from the measured values by 51- $\sigma$  and 22- $\sigma$ , respectively, easily ruling out the background hypothesis. Instead, our second epoch astrometry is much closer to the first epoch measurements, differing by  $15.0 \pm 0.2$  mas and  $1.96 \pm 0.11^\circ$ . This difference is plausibly explained by orbital motion.

While this rules out contamination from a stationary background object, there is a small (but non-zero) probability that the candidate companion is an unassociated star with coincident sky position and proper motion. We approach this problem in two ways: (1) by calculating the *a priori* probability of a chance alignment of a field ultracool dwarf regardless of any information about proper motions, and (2) using a galaxy model to derive the expected contamination rate of background stars with proper motions similar to GJ 3629.

The probability of an ultracool dwarf falling in the NIRC2 field of view can be computed from the surface density of ultracool dwarfs ( $\Sigma_{UC}$ ) and the solid angle

subtended by the instrument ( $\Omega$ ). The most complete census of ultracool dwarfs within 20 pc was compiled by Reid et al. (2008). They identified 196 M7–T2.5 systems covering  $\approx 65\%$  of the celestial sphere, which corresponds to a surface density  $\Sigma_{UC}$  of  $\sim 7.3 \times 10^{-3} \text{ deg}^{-2}$ . Our short exposure images of the GJ 3629 A reach  $\Delta J \sim 7$ , or  $J \sim 16.4$  mag. This is comparable to the limiting magnitude of the 2MASS survey from which the Reid et al. compilation is based, so no correction to the surface density is needed since the same depth is probed. The Poisson distribution gives the probability of observing an event given an expectation value ( $\Sigma_{UC} \times \Omega$ ). Since this value is small, the probability converges to the expectation value itself, which is  $\sim 6 \times 10^{-8}$  for the  $10''2 \times 10''2$  NIRC2 narrow camera. GJ 3629 is part of our larger PALMS imaging survey, so the total sample size of the survey must be taken into account to determine if this rare event is consistent with the expected contamination rate for a given number of trials. When the multi-band observations of GJ 3629 AB were made, which identified the candidate companion as a late-type object, we had imaged about 100 M dwarfs. Assuming the contamination rate for the survey is comparable to that of GJ 3629, the probability of a field ultracool dwarf falling within our field of view by chance is roughly  $6 \times 10^{-6}$ . Note that this only assumes contamination from a foreground ultracool dwarf without incorporating background late-type giants (which will increase the probability of contamination); the coincident proper motions of the components were also not taken into account (which will decrease the probability of contamination).

We also estimate the probability of contamination by a background star using the TRILEGAL population synthesis code (Girardi et al. 2005). Here we use the default settings for the initial mass function, binary statistics, extinction values, and components of the galaxy. We queried a  $10 \text{ deg}^2$  region of the sky at the position of GJ 3629 in the MKO filter system down to a depth of 26 mag in  $H$  band (L. Girardi, private communication). For the purposes of this *a posteriori* calculation, the magnitude cutoffs must reflect a range that would have been deemed “interesting” and worthy of follow-up observations. This corresponds to substellar objects down to the detection limits of our Keck short exposure images. Given the distance ( $\sim 22$  pc) and age ( $\sim 100$  Myr) of GJ 3629, the Baraffe et al. (2003) evolutionary models give a substellar brightness cutoff of  $J=11.4$ . The surface density of stars with  $11.4 < J < 16.4$  from the models is  $62 \text{ deg}^{-2}$ , implying a probability of  $\sim 5 \times 10^{-4}$  of a background star falling in the field of view. TRILEGAL also includes a kinematic model that predicts stellar proper motions and has been shown to reproduce observed proper motion distributions (Rossetto et al. 2011). If in addition to our magnitude cutoff we impose a proper motion constraint of  $\pm 30 \text{ mas/yr}$  in  $\mu_\alpha \cos \delta$  and  $\mu_\delta$  from GJ 3629, the implied surface density is  $0.01 \text{ deg}^{-2}$  and the probability of contamination is  $\sim 8 \times 10^{-8}$ . (This loose proper motion constraint allows for some orbital motion at smaller separations.) Note that we have not included a color cutoff; this probability is for all background stars. Even with the sample size of 100 targets, the probability that the candidate companion is a background object is negligibly small. GJ 3629 B is therefore

physically bound to the primary, and we can expect a third epoch of astrometry in a few years to show evidence of curvature in the orbital motion.

### 3.3. Age

X-ray and UV emission can be used to infer the ages of solar-type stars down to stars near the fully-convective boundary since high-energy emission traces magnetic field strengths, which decay over time as a result of slowing rotation rates (e.g., Skumanich 1972; Preibisch & Feigelson 2005). GJ 3629 AB is detected in the *ROSAT* All Sky Bright-Source Catalog (Voges et al. 1999) and both the near-UV (NUV) and far-UV (FUV) bands of the *Galaxy Evolution Explorer* (*GALEX*; Martin et al. 2005) space telescope as part of its All-sky Imaging Survey (Morrissey et al. 2007).

The measured count rate from *ROSAT* is  $0.127 \pm 0.022 \text{ sec}^{-1}$  with hardness ratios from the Position Sensitive Proportional Counter instrument of  $HR1 = -0.02 \pm 0.16$  and  $HR2 = -0.40 \pm 0.20$ . This corresponds to an X-ray flux of  $1.0 \pm 0.2 \times 10^{-12} \text{ erg s}^{-1} \text{ cm}^{-2}$  using the conversion factor from Fleming et al. (1995), which uses the  $HR1$  measurement as a proxy for the shape of the X-ray spectrum. Assuming a distance of  $22 \pm 3$  pc, GJ 3629 AB has an X-ray luminosity of  $\log L_X = 28.8 \pm 0.2 \text{ erg s}^{-1}$ . We calculate a fractional luminosity (which is independent of distance) of  $\log(L_X/L_{\text{Bol}}) = -2.90 \pm 0.10$  using the  $H$ -band bolometric correction from Casagrande et al. (2008). Compared to the cumulative distributions of X-ray luminosities and fractional luminosities for young clusters from Preibisch & Feigelson (2005), the values for GJ 3629 AB are comparable to cluster members with ages younger than the Hyades (625 Myr). The large fractional X-ray luminosity is in the saturated regime where M dwarfs cease to emit higher X-ray fluxes even with faster rotation rates (Delfosse et al. 1998; Pizzolato et al. 2003; Wright et al. 2011). Shkolnik et al. (2009) derive an X-ray to  $J$ -band fractional luminosity of  $-2.19$ , which is likewise higher than nearly all Hyades members for that color. The hardness ratios also appear to be closer to those of young moving group members and Hyades members than the softer values of the field population (Kastner et al. 2003).

Several studies have noted that young stars separate themselves from old field dwarfs in a variety of *GALEX*-NIR/optical colors (Findeisen & Hillenbrand 2010; Shkolnik et al. 2011; Rodriguez et al. 2011; Findeisen et al. 2011; Schlieder et al. 2012). Figure 3 shows the location of Hyades ( $\sim 625$  Myr), Blanco 1 ( $\sim 100$  Myr), AB Dor ( $\sim 100$  Myr), Tuc/Hor ( $\sim 30$  Myr),  $\beta$  Pic ( $\sim 12$  Myr), and TW Hya ( $\sim 8$  Myr) members in the  $NUV-J$  vs.  $J-K_S$  and  $FUV-J$  vs.  $J-K_S$  diagrams from Findeisen et al. (2011). The Hyades trace an upper red envelope with younger stars generally having bluer  $NUV-J$  and  $FUV-J$  colors. The photometry for GJ 3629 AB (Table 3) fall  $\sim 1$  mag below this sequence and have similar colors to M-type members of the  $\beta$  Pic moving group in both diagrams. However, we note that the lack of Li observed by Shkolnik et al. (2009) places a lower limit to the age  $\sim 25$  Myr based on the Li depletion models of Chabrier et al. (1996). The *GALEX* data therefore bolster a young age for GJ 3629 AB as indicated by its X-ray emission but do not provide any tighter

age constraints; we therefore adopt the 25–300 Myr age suggested by Shkolnik et al. (2009) for this work. The *UVW* kinematics and *XYZ* position of GJ 3629 AB (Table 4) based on the measured radial velocity of the system (Shkolnik et al. 2012, ApJ, submitted) do not appear to match those of any known young moving groups.

Since rotation rates decay over time, in principle it should be possible to infer ages from rotation periods by empirically calibrating them to well-studied coeval clusters. It has become clear in recent years, however, that stars are born with a large range of rotation periods that evolve non-uniformly (e.g., Stassun et al. 1999). This is particularly true of M dwarfs with fully convective interiors ( $M \lesssim 0.3 M_{\odot}$ , SpT  $\gtrsim$  M4), whose periods increase between  $\sim 10$  and 200 Myr as they contract to the zero-age main sequence and then exhibit a large spread in ages at  $\gtrsim 1$  Gyr (Irwin et al. 2011). Hartman et al. (2011) measured a rotation period for GJ 3629 A of 3.78 days as part of the HATNet project to find transiting extrasolar planets (Bakos et al. 2004). With a mass of  $\sim 0.25 M_{\odot}$  (Section 3.5), GJ 3629 A sits near the edge of this fully convective boundary, and based on the compilation of open cluster data from Irwin et al. (2011) the age cannot be constrained from its rotation period alone.

Finally, we note that an upper limit for the age of the system can be estimated using the typical activity lifetimes for M dwarf revealed through  $H\alpha$  emission. Shkolnik et al. (2009) detected  $H\alpha$  emission ( $EW = -3 \text{ \AA}$ ) in GJ 3629 A, which implies an age of  $\lesssim 2$  Gyr given the spectral type-activity lifetime relations derived by West et al. (2008). This provides further support that the system is young.

#### 3.4. Spectral Type

We use the resolved photometry of GJ 3629 AB to estimate the spectral type of the companion. Figure 4 shows the positions of GJ 3629 A and B in *YJHK* color-color diagrams relative to dwarfs (blue) and giants (orange) from Cushing et al. (2005) and Rayner et al. (2009). For the *Y*-band magnitude of the primary we use the mean of the *Y*–*J* color from the two M3V dwarfs in Rayner et al. (2009) combined with the *J*-band magnitude of the primary. The *Y*-band magnitude of the companion is then computed from our relative photometry for the system. We estimate the intrinsic uncertainty in *Y*–*J* color as half the difference of those from the two M3V objects. The *J*–*H* color of GJ 3629 B is similar to that of the primary, but the companion is redder in both *Y*–*J* and *H*–*K*. Figure 5 shows *Y*–*J* and *H*–*K* colors versus spectral type for the same comparison objects. The *Y*–*J* color of GJ 3629 B suggests a classification of  $M7 \pm 2$ ; its *H*–*K* color is less constraining at  $M6 \pm 4$ . We therefore adopt a spectral type of  $M7 \pm 2$  for the companion.

#### 3.5. Physical Properties

We derive a luminosity of  $\log(L_{\text{Bol}}/L_{\odot}) = -1.90 \pm 0.13$  for the M3.0 primary GJ 3629 A using the *H*-band bolometric correction from Casagrande et al. (2008) and a distance estimate of  $22 \pm 3$  pc. At 30, 100, and 300 Myr, the evolutionary models of Baraffe et al. (1998) imply masses of  $\sim 0.15$ , 0.25, and  $0.30 M_{\odot}$  and effective temperatures of  $\sim 3120$ , 3370, and 3440 K, respectively. Because of the uncertainty in age and distance, we assume a mass of  $0.25 \pm 0.05 M_{\odot}$  for the primary GJ 3629 A.

We estimate a luminosity for GJ 3629 B using the *K*-band bolometric corrections from Liu et al. (2010a), arriving at a value of  $\log(L_{\text{Bol}}/L_{\odot}) = -3.23 \pm 0.14$  assuming a distance of  $22 \pm 3$  and a spectral type of  $M7 \pm 2$ . This translates into a mass of  $46 \pm 16 M_{\text{Jup}}$  based on an interpolated grid of substellar models from Burrows et al. (1997) as shown in Figure 6. Similar masses are obtained using the brown dwarf evolutionary models of Chabrier et al. (2000), Baraffe et al. (2003), and Saumon & Marley (2008).

## 4. DISCUSSION AND CONCLUSIONS

With an angular separation of  $\approx 200$  mas, GJ 3629 AB has a projected physical separation of  $4.4 \pm 0.6$  AU at a distance of  $22 \pm 3$  pc. Dupuy & Liu (2011) calculate statistical correction factors to convert projected separations of visual binaries into semimajor axes using a variety of input eccentricity distributions. Assuming their conversion factor of 1.16, which represents the case of no discovery bias and an input eccentricity distribution from the observed population of very low-mass binaries, we estimate the orbital period of the GJ 3629 AB system to be  $21 \pm 5$  yr. This raises the possibility of measuring a dynamical mass for the system on a modest timescale. Radial velocity monitoring of the system will also be feasible because the velocity semi-amplitude induced by the companion is expected to be  $\sim 1.0 \text{ km s}^{-1}$  assuming an inclination of  $90^{\circ}$ . A parallax measurement and continuing astrometric and radial velocity monitoring should be a high priority for this system.

A growing list of brown dwarfs now have dynamical mass measurements (e.g., Liu et al. 2008; Dupuy et al. 2010; Konopacky et al. 2010), but very few of these also have good age and metallicity constraints from being companions to well-characterized stars or members of coeval clusters. This rare class of brown dwarfs—representing both “age benchmarks” and “mass benchmarks”—functions as an excellent tool to accurately test substellar evolutionary models (Liu et al. 2008). For example, Dupuy et al. (2009) measured the dynamical mass of the binary brown dwarf HD 130948 BC and used the precise age determination of the primary star ( $0.8 \pm 0.2$  Gyr) to test two of the most commonly used substellar cooling models (Burrows et al. 1997; Chabrier et al. 2000). They found that these models underpredict the luminosities of HD 130948 BC by a factor of 2–3. Other brown dwarfs with dynamical masses and well-constrained “environmental” ages (that is, not dependent on substellar cooling models) are the young ( $\sim 1$  Myr) eclipsing binary brown dwarf pair 2MASS J05352184–0546085 AB (Stassun et al. 2006) and the  $2.2 \pm 1.5$  Gyr system HR 7672 B (Liu et al. 2002; Crepp et al. 2011).<sup>6</sup> Many of the aforementioned

<sup>6</sup> The other systems consisting of one or more brown dwarfs with a dynamical mass measurement and a stellar primary all have poor age constraints. The triple system GJ 569 Bab (Martin et al. 2000; Lane et al. 2001) appears to have an age  $\lesssim 1$  Gyr but the estimates for the primary star vary widely in the literature (see Dupuy et al. 2010 for a summary). Likewise, various age estimates for the  $\epsilon$  Indi Bab triple system (Scholz et al. 2003; Mccaughrean et al. 2004; Cardoso et al. 2009) place it between  $\sim 0.5$ –7 Gyr (see Liu et al. 2010a and King et al. 2010). The triple system GJ 802 AB (Pravdo et al. 2005; Lloyd et al. 2006) also has a dynamical mass measurement (Ireland et al. 2008), but the age constraint based on its kinematics is rather weak at  $\sim 3$ –10 Gyr.

benchmarks used unique methods to extract individual masses for the system components. For example, Dupuy et al. (2009) relied on the HD 130948 BC companions having nearly equal flux ratios to infer relative masses; Stassun et al. (2006) used the well-constrained inclination of the eclipsing binary 2MASS J05352184–0546085 AB to extract individual masses from radial velocity curves; and Crepp et al. (2011) used radial velocity data of the primary star and visual orbit monitoring of the companion to infer the mass of the HR 7672 B.

For GJ 3629 AB to join this rare group of benchmarks, individual masses will have to be measured instead of a total mass for the system, which is what relative orbit monitoring yields. A stationary point source is visible  $\sim 30''$  north of GJ 3629 AB in POSS-I and POSS-II images from the Digitized Sky Surveys, but it is not detected by 2MASS. The source (SDSS J105120.51+360752.3) was identified by Schneider et al. (2007) as a quasar based on optical spectroscopy from the Sloan Digital Sky Survey (SDSS). Its optical colors from SDSS are very blue, but with a  $z$ -band magnitude of 18.8 mag it should be possible to use this as a reference object in the near-infrared for absolute astrometry of the GJ 3629 AB system. Finally, we note that several observations can be made to further refine the age of the GJ 3629 AB system: a parallax measurement would enable placement on the HR diagram and resolved near-infrared spectroscopy of GJ 3629 B would provide age constraints though the use of gravity-sensitive features (e.g., Allers et al. 2007). Altogether, GJ 3629 AB represents a promising system for future studies.

We thank our anonymous referee for helpful comments, Michael Cushing for providing the synthetic photometry for L dwarfs, Krzysztof Findeisen for the *GALEX* photometry of young moving group members, and Léo Girardi for the TRILEGAL results. BPB and MCL have been supported by NASA grant NNX11AC31G and NSF grant AST09-09222. MT is supported by a Grant-in-Aid for Science Research in a Priority Area from MEXT. It is a pleasure to thank our Keck support astronomer Hien Tran and observing assistant Jason McIlroy for their help in making this work possible. We utilized data products from the Two Micron All Sky Survey, which is a joint project of the University of Massachusetts and the Infrared Processing and Analysis Center/California Institute of Technology, funded by the National Aeronautics and Space Administration and the National Science Foundation. NASA’s Astrophysics Data System Bibliographic Services together with the VizieR catalogue access tool and SIMBAD database operated at CDS, Strasbourg, France, were invaluable resources for this work. The National Geographic Society-Palomar Observatory Sky Atlas (POSS-I) was made by the California Institute of Technology with grants from the National Geographic Society. The Second Palomar Observatory Sky Survey (POSS-II) was made by the California Institute of Technology with funds from the National Science Foundation, the National Geographic Society, the Sloan Foundation, the Samuel Oschin Foundation, and the Eastman Kodak Corporation. The Digitized Sky Surveys were produced at the Space Telescope Science Institute under

U.S. Government grant NAG W-2166. The images of these surveys are based on photographic data obtained using the Oschin Schmidt Telescope on Palomar Mountain and the UK Schmidt Telescope. The plates were processed into the present compressed digital form with the permission of these institutions. Finally, mahalo nui loa to the kama‘āina of Hawai‘i for their support of Keck and the Mauna Kea observatories. We are grateful to conduct observations from this mountain.

*Facilities:* Keck:II (NIRC2)

## REFERENCES

- Allers, K. N., et al. 2007, *ApJ*, 657, 511
- Bakos, G., Noyes, R. W., Kovács, G., Stanek, K. Z., Sasselov, D. D., & Domsa, I. 2004, *PASP*, 116, 266
- Baraffe, I., Chabrier, G., Allard, F., & Hauschildt, P. H. 1998, *A&A*, 337, 403
- Baraffe, I., Chabrier, G., Barman, T. S., Allard, F., & Hauschildt, P. H. 2003, *A&A*, 402, 701
- Biller, B. A., et al. 2007, *ApJSS*, 173, 143
- Bochanski, J. J., Hawley, S. L., Covey, K. R., West, A. A., Reid, I. N., Golimowski, D. A., & Ivezić, Z. 2010, *AJ*, 139, 2679
- Bowler, B. P., et al. 2010, *ApJ*, 709, 396
- Bowler, B. P., Liu, M. C., Kraus, A. L., Mann, A. W., & Ireland, M. J. 2011, *ApJ*, 743, 148
- Bowler, B. P., Liu, M. C., Shkolnik, E. L., Dupuy, T. J., Cieza, L. A., Kraus, A. L., & Tamura, M. 2012, *arXiv/astro-ph*: 1205.2084
- Burrows, A., Hubbard, W. B., Lunine, J. I., & Liebert, J. 2001, *Reviews of Modern Physics*, 73, 719
- Burrows, A., et al. 1997, *ApJ*, 491, 856
- Cardoso, C. V., et al. 2009, in *AIP Conf. Proc* 1094, 15th Cambridge Workshop on CoolStars, Stellar Systems and the Sun, ed. E. Stempels (Melville, NY: AIP), 509
- Casagrande, L., Flynn, C., & Bessell, M. 2008, *MNRAS*, 389, 585
- Chabrier, G., Baraffe, I., Allard, F., & Hauschildt, P. 2000, *ApJ*, 542, 464
- Chabrier, G., Baraffe, I., & Plez, B. 1996, *Astrophysical Journal Letters* v.459, 459, L91
- Crepp, J. R., et al. 2011, *arXiv/astro-ph*: 1112.1725, *astro-ph.EP*
- Cushing, M. C., Rayner, J. T., & Vacca, W. D. 2005, *ApJ*, 623, 1115
- Delfosse, X., Forveille, T., Perrier, C., & Mayor, M. 1998, *A&A*, 331, 581
- Dupuy, T. J., & Liu, M. C. 2011, *ApJ*, 733, 122
- Dupuy, T. J., Liu, M. C., Bowler, B. P., Cushing, M. C., Helling, C., Witte, S., & Hauschildt, P. 2010, *ApJ*, 721, 1725
- Dupuy, T. J., Liu, M. C., & Ireland, M. J. 2009, *ApJ*, 692, 729
- Findeisen, K., & Hillenbrand, L. 2010, *AJ*, 139, 1338
- Findeisen, K., Hillenbrand, L., & Soderblom, D. 2011, *AJ*, 142, 23
- Fleming, T. A., Molendi, S., Maccacaro, T., & Wolter, A. 1995, *Astrophysical Journal Supplement* v.99, 99, 701
- Girardi, L., Groenewegen, M. A. T., Hatziminaoglou, E., & Costa, L. D. 2005, *A&A*, 436, 895
- Goldman, B., Marsat, S., Henning, T., Clemens, C., & Greiner, J. 2010, *MNRAS*, 405, 1140
- Hartman, J. D., Bakos, G. Á., Noyes, R. W., Sipócz, B., Kovács, G., Mazeh, T., Shporer, A., & Pál, A. 2011, *AJ*, 141, 166
- Henry, T. J., Ianna, P. A., Kirkpatrick, J. D., & Jahreiss, H. 1997, *Astron. J.* 114, 114, 388
- Ireland, M. J., Kraus, A., Martinache, F., Law, N., & Hillenbrand, L. A. 2011, *ApJ*, 726, 113
- Ireland, M. J., Kraus, A., Martinache, F., Lloyd, J. P., & Tuthill, P. G. 2008, *ApJ*, 678, 463
- Irwin, J., Berta, Z. K., Burke, C. J., Charbonneau, D., Nutzman, P., West, A. A., & Falco, E. E. 2011, *ApJ*, 727, 56
- Janson, M., Carson, J. C., Lafrenière, D., Spiegel, D. S., Bent, J. R., & Wong, P. 2012, *ApJ*, 747, 116
- Johnson, J. A., Aller, K. M., Howard, A. W., & Crepp, J. R. 2010, *PASP*, 122, 905
- Johnson, J. A., Butler, R. P., Marcy, G. W., Fischer, D. A., Vogt, S. S., Wright, J. T., & Peek, K. M. G. 2007, *ApJ*, 670, 833
- Kalas, P., et al. 2008, *Science*, 322, 1345
- Kastner, J. H., Crigger, L., Rich, M., & Weintraub, D. A. 2003, *ApJ*, 585, 878
- King, R. R., McCaughrean, M. J., Homeier, D., Allard, F., Scholz, R.-D., & Lodieu, N. 2010, *A&A*, 510, 99
- Konopacky, Q. M., Ghez, A. M., Barman, T. S., Rice, E. L., Bailey, J. I., White, R. J., McLean, I. S., & Duchêne, G. 2010, *ApJ*, 711, 1087
- Kraus, A. L., & Ireland, M. J. 2012, *ApJ*, 745, 5
- Lafrenière, D., et al. 2007, *ApJ*, 670, 1367
- Lafrenière, D., Jayawardhana, R., & van Kerkwijk, M. H. 2008, *ApJ*, 689, L153
- Lagrange, A.-M., et al. 2010, *Science*, 329, 57
- . 2009, *A&A*, 493, L21
- Lane, B. F., Osorio, M. R. Z., Britton, M. C., Martín, E. L., & Kulkarni, S. R. 2001, *ApJ*, 560, 390
- Leggett, S. K., et al. 2006, *MNRAS*, 373, 781
- Lépine, S., & Gaidos, E. 2011, *AJ*, 142, 138
- Lépine, S., & Shara, M. M. 2005, *AJ*, 129, 1483
- Liu, M. C., Dupuy, T. J., & Ireland, M. J. 2008, *ApJ*, 689, 436
- Liu, M. C., Dupuy, T. J., & Leggett, S. K. 2010a, *ApJ*, 722, 311
- Liu, M. C., Fischer, D. A., Graham, J. R., Lloyd, J. P., Marcy, G. W., & Butler, R. P. 2002, *ApJ*, 571, 519
- Liu, M. C., et al. 2010b, *Adaptive Optics Systems II*. Edited by Ellerbroek, 7736, 53
- Lloyd, J. P., Martinache, F., Ireland, M. J., Monnier, J. D., Pravdo, S. H., Shaklan, S. B., & Tuthill, P. G. 2006, *ApJ*, 650, L131
- Lovis, C., & Mayor, M. 2007, *A&A*, 472, 657
- Lowrance, P. J., et al. 2005, *AJ*, 130, 1845
- Luhman, K. L., Burgasser, A. J., & Bochanski, J. J. 2011, *ApJ*, 730, L9
- Lupton, R., Blanton, M. R., Fekete, G., Hogg, D. W., O'Mullane, W., Szalay, A., & Wherry, N. 2004, *PASP*, 116, 133
- Marengo, M., Stapelfeldt, K., Werner, M. W., Hora, J. L., Fazio, G. G., Schuster, M. T., Carson, J. C., & Megeath, S. T. 2009, *ApJ*, 700, 1647
- Marois, C., Lafrenière, D., Macintosh, B., & Doyon, R. 2008, *ApJ*, 673, 647
- Marois, C., Zuckerman, B., Konopacky, Q. M., Macintosh, B., & Barman, T. 2010, *Nature*, 468, 1080
- Martin, D. C., et al. 2005, *ApJ*, 619, L1
- Martín, E. L., Koresko, C. D., Kulkarni, S. R., Lane, B. F., & Wizinowich, P. L. 2000, *ApJ*, 529, L37
- McCaughrean, M. J., Close, L. M., Scholz, R.-D., Lenzen, R., Biller, B., Brandner, W., Hartung, M., & Lodieu, N. 2004, *A&A*, 413, 1029
- Monet, D. G., et al. 2003, *AJ*, 125, 984
- Morrissey, P., et al. 2007, *ApJSS*, 173, 682
- Pizzolato, N., Maggio, A., Micela, G., Sciortino, S., & Ventura, P. 2003, *A&A*, 397, 147
- Pravdo, S. H., Shaklan, S. B., & Lloyd, J. 2005, *ApJ*, 630, 528
- Preibisch, T., & Feigelson, E. D. 2005, *ApJSS*, 160, 390
- Rayner, J. T., Cushing, M. C., & Vacca, W. D. 2009, *ApJSS*, 185, 289
- Reid, I. N., et al. 2004, *AJ*, 128, 463
- Reid, I. N., Cruz, K. L., Kirkpatrick, J. D., Allen, P. R., Mungall, F., Liebert, J., Lowrance, P., & Sweet, A. 2008, *AJ*, 136, 1290
- Reid, I. N., Hawley, S. L., & Gizis, J. E. 1995, *AJ*, 110, 1838
- Rodríguez, D. R., Bessell, M. S., Zuckerman, B., & Kastner, J. H. 2011, *ApJ*, 727, 62
- Rossetto, B. M., et al. 2011, *AJ*, 141, 185
- Saumon, D., & Marley, M. S. 2008, *ApJ*, 689, 1327
- Schlieder, J. E., Lépine, S., & Simon, M. 2012, *AJ*, 143, 80
- Schneider, D. P., et al. 2007, *AJ*, 134, 102
- Scholz, R.-D. 2010, *A&A*, 515, A92
- Scholz, R.-D., McCaughrean, M. J., Lodieu, N., & Kuhlbrodt, B. 2003, *A&A*, 398, L29
- Shkolnik, E., Liu, M. C., & Reid, I. N. 2009, *ApJ*, 699, 649
- Shkolnik, E. L., Liu, M. C., Reid, I. N., Dupuy, T., & Weinberger, A. J. 2011, *ApJ*, 727, 6
- Siess, L., Dufour, E., & Forestini, M. 2000, *A&A*, 358, 593
- Simons, D. A., & Tokunaga, A. 2002, *PASP*, 114, 169
- Skrutskie, M. F., et al. 2006, *AJ*, 131, 1163
- Skumanich, A. 1972, *ApJ*, 171, 565
- Stassun, K. G., Mathieu, R. D., Mazeh, T., & Vrba, F. J. 1999, *AJ*, 117, 2941
- Stassun, K. G., Mathieu, R. D., & Valenti, J. A. 2006, *Nature*, 440, 311
- Tokunaga, A. T., & Vacca, W. D. 2005, *PASP*, 117, 421
- Voges, W., et al. 1999, *A&A*, 349, 389
- West, A. A., Hawley, S. L., Bochanski, J. J., Covey, K. R., Reid, I. N., Dhital, S., Hilton, E. J., & Masuda, M. 2008, *AJ*, 135, 785
- Wizinowich, P., et al. 2000, *PASP*, 112, 315
- Wright, N. J., Drake, J. J., Mamajek, E. E., & Henry, G. W. 2011, *ApJ*, 743, 48
- Yelda, S., Lu, J. R., Ghez, A. M., Clarkson, W., Anderson, J., Do, T., & Matthews, K. 2010, *ApJ*, 725, 331

Zacharias, N., Monet, D. G., Levine, S. E., Urban, S. E., Gaume, R., & Wycoff, G. L. 2005, *VizieR On-line Data Catalog*, 1297, 0

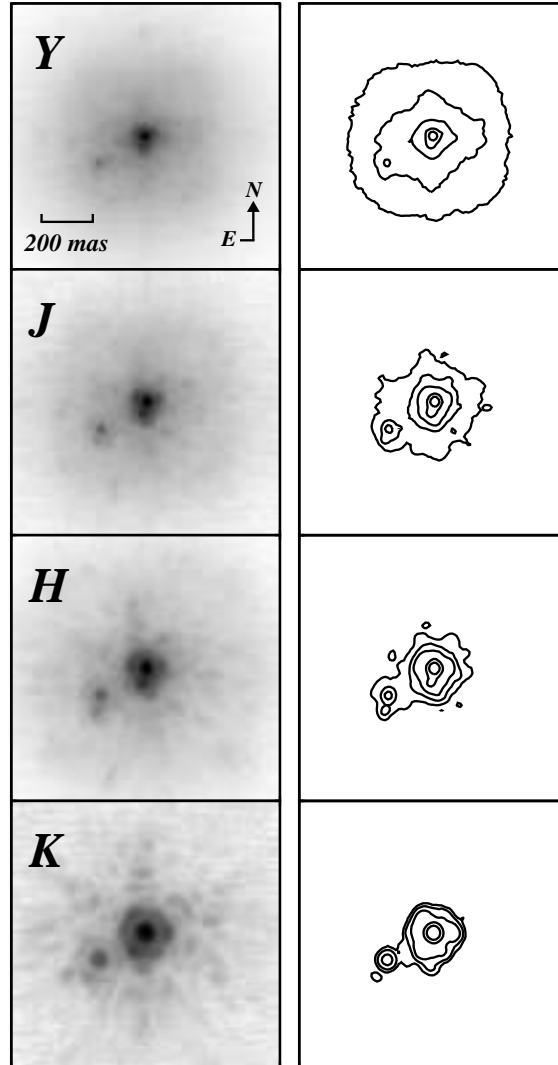


FIG. 1.— Keck-II/NIRC2 *YJHK* images of GJ 3629 AB. The left panels show coadded frames of the system with an asinh stretch to bring out faint features (Lupton et al. 2004). The right panels show contours representing 50%, 20%, 5%, 2%, and 1% of the peak flux from the primary. Artifacts from the AO correction during the poor second epoch conditions are visible below the real point sources, especially in the *J*- and *H*-band frames. North is up and East is left in the images.



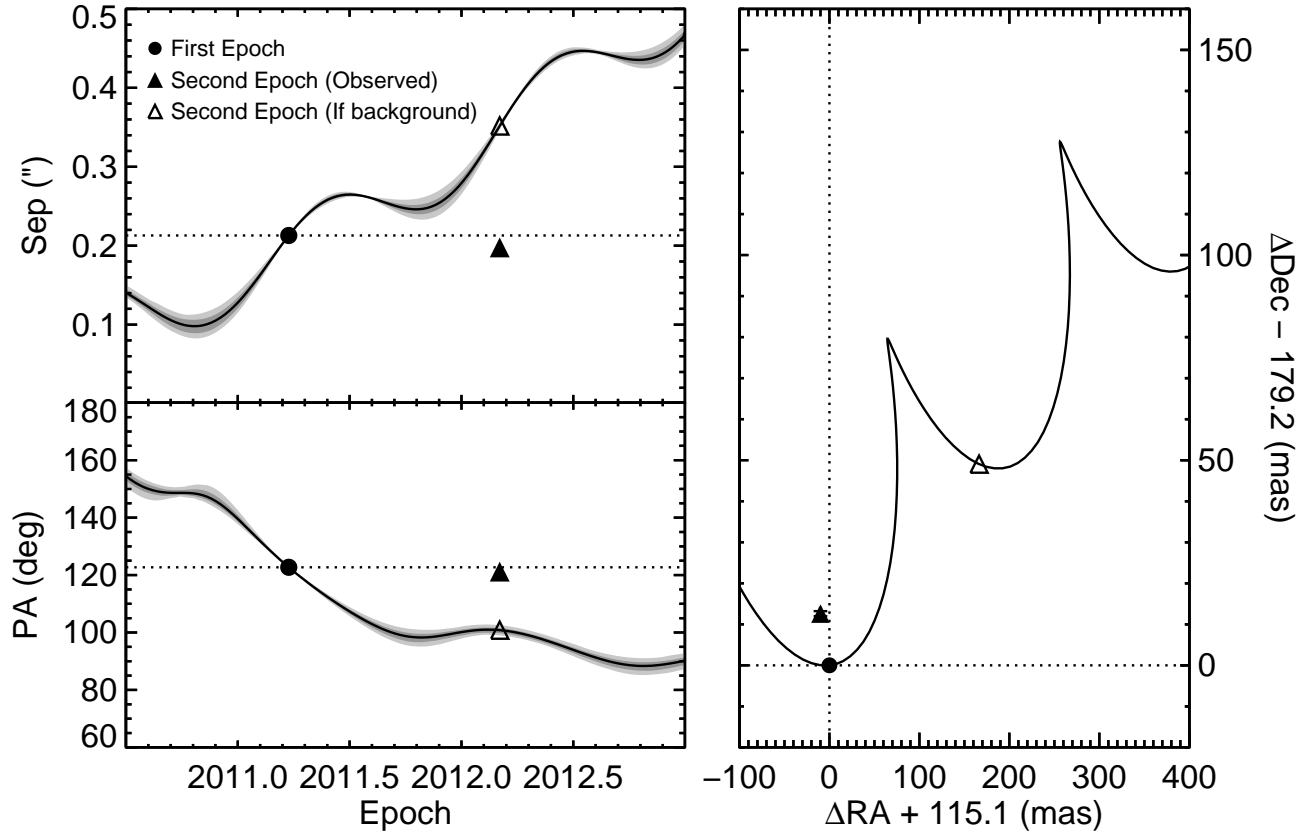


FIG. 2.— Predicted relative motion of a stationary object at the first epoch position (filled circle) of the companion to GJ 3629 A. The left panels show the change in separation and position angle over time due to the parallax and proper motion of the primary. Gray 1- and 2- $\sigma$  shaded confidence intervals incorporate uncertainties in the proper motion, distance estimate ( $22 \pm 3$  pc), and first epoch astrometry. The right panel shows the motion in relative RA and Dec offsets ( $\Delta$  refers to primary – secondary position). Our second epoch measurement (filled triangle) rules out the background hypothesis (open triangle) and shows the companion shares nearly common proper motion with the primary, with the slight difference between epochs attributable to orbital motion. The astrometric measurement uncertainties are smaller than the size of the symbols.

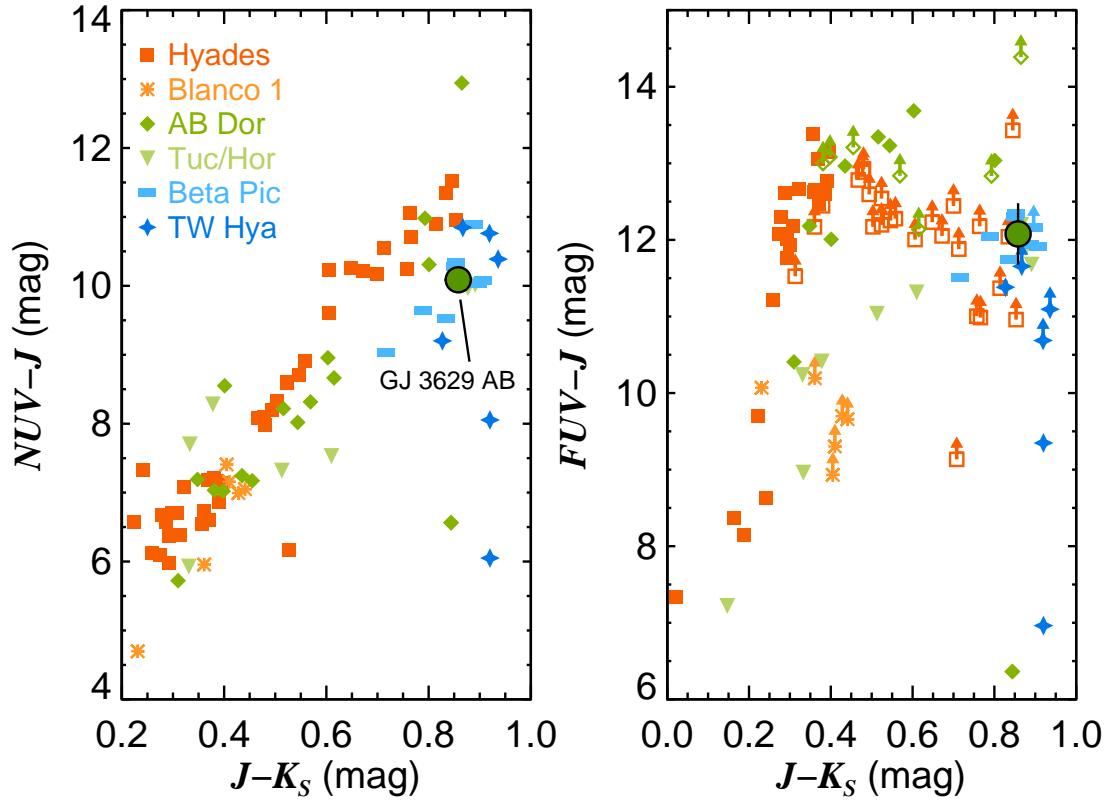


FIG. 3.— *GALEX*  $NUV-J$  (left) and  $FUV-J$  (right) colors as a function of  $J-K_S$  for young clusters between  $\sim 8$  Myr (TW Hya) and  $\sim 625$  Myr (Hyades). Young stars tend to have blue UV-NIR colors, generally falling below the Hyades sequence. GJ 3629 AB (green filled circle) sits  $\sim 1$  mag below this envelope in  $NUV-J$  and appears to have an age confidently less than the Hyades. Photometry for the cluster members are from Findeisen et al. (2011); open symbols and upward arrows indicate lower limits.

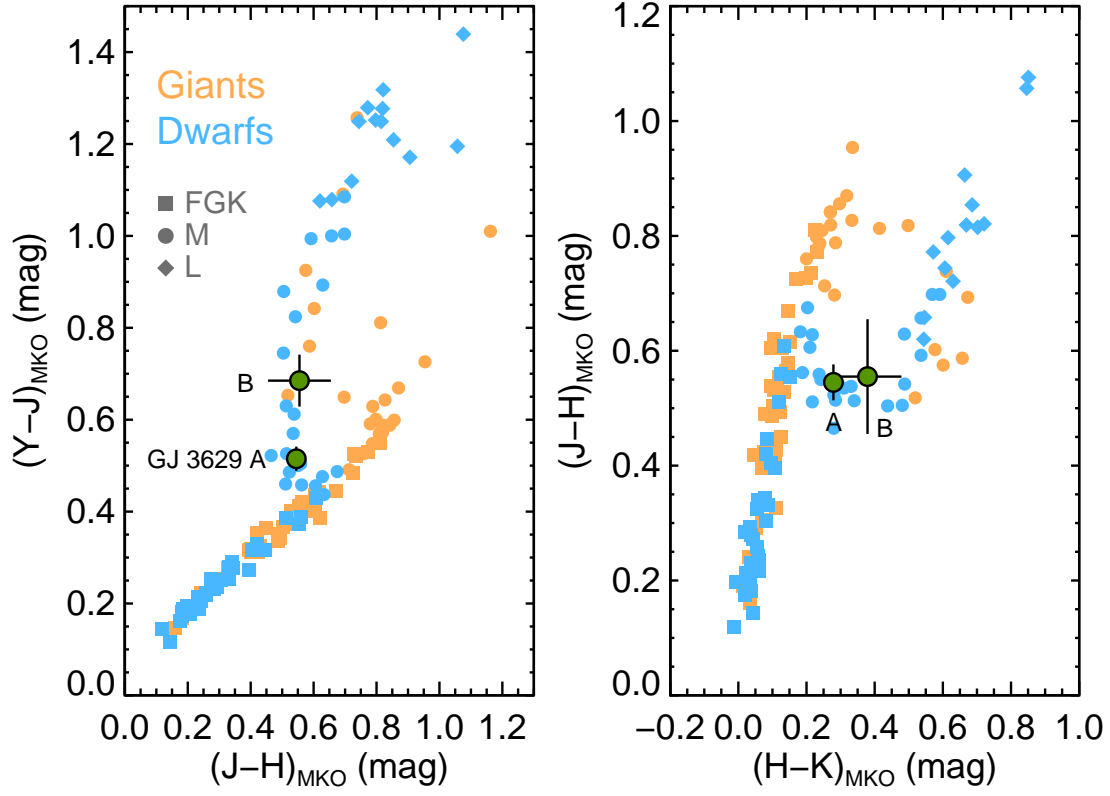


FIG. 4.— Near-infrared color-color diagrams showing the positions of GJ3629 A and B (solid green circles) relative to dwarfs (blue) and giants (orange). GJ 3629 B is redder in  $Y - J$  (left) and  $H - K$  (right) than the primary and has colors comparable to M6–M7 dwarfs. The FGK (squares) and M (circles) dwarf and giant data are synthesized MKO photometry from Rayner et al. (2009) and the late-M and L dwarfs are from Cushing et al. (2005).

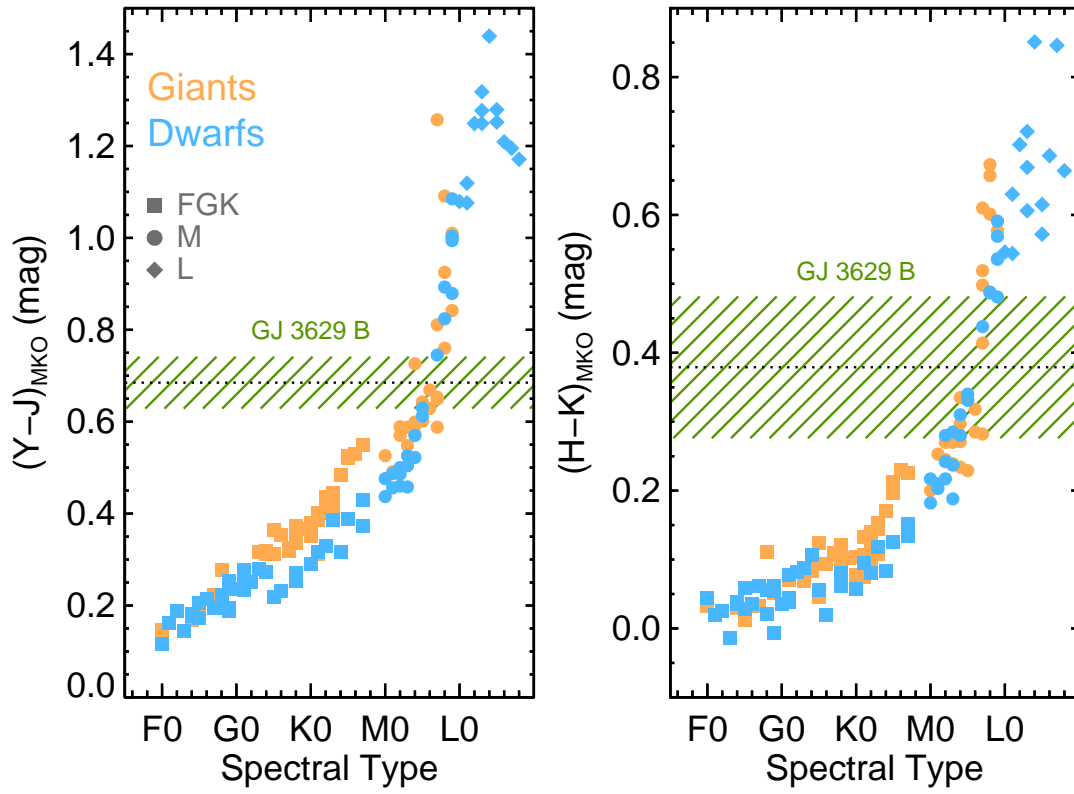


FIG. 5.— Near-infrared colors for giants (orange) and dwarfs (blue) as a function of spectral type. The  $Y-J$  (left) and  $H-K$  (right) colors of GJ 3629 B suggest a spectral type of  $M7 \pm 2$  and  $M6 \pm 4$ , respectively. Photometry for the dwarfs and giants are from Rayner et al. (2009) and Cushing et al. (2005).

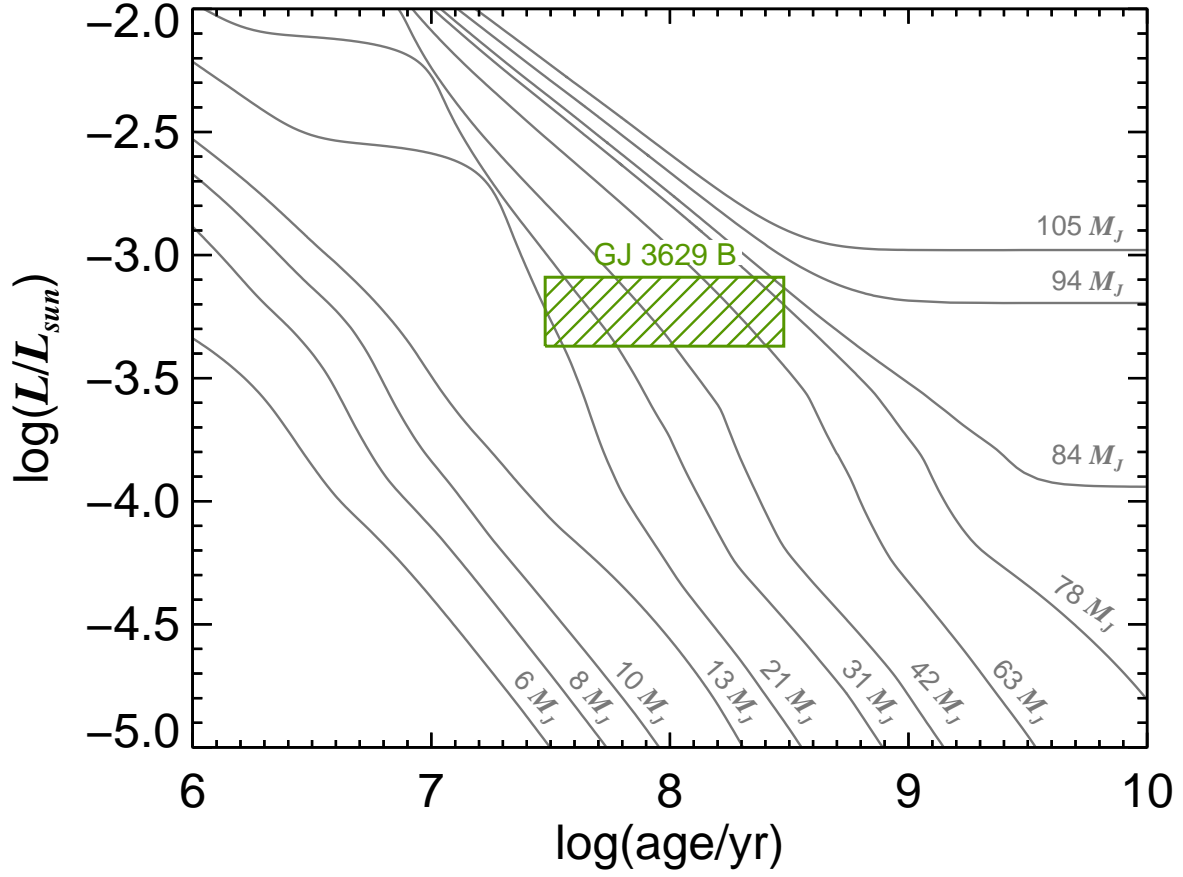


FIG. 6.— Mass estimate for GJ 3629 B based on the evolutionary models of Burrows et al. (1997). The green region shows the model predictions for the age (25–300 Myr) and estimated distance ( $22 \pm 3$  pc) of the primary, which yields  $46 \pm 16 M_{Jup}$  for GJ 3629 B. This is well below the hydrogen burning limit ( $\sim 78 M_{Jup}$ ; e.g. Burrows et al. 2001).

TABLE 1  
KECK-II/NIRC2 OBSERVATIONS

UT Date (Y/M/D)	Filter	No. of Exposures	Coadds $\times$ Exp. Time (s)
2011/03/25	$K_S$	3	100 $\times$ 0.11
2012/03/03	$Y$	9	20 $\times$ 1.0
2012/03/03	$J$	12	20 $\times$ 0.11
2012/03/03	$H$	20	20 $\times$ 0.11
2012/03/03	$K$	20	10 $\times$ 0.11

TABLE 2  
KECK-II/NIRC2 ASTROMETRY OF GJ 3629 AB

Epoch (UT)	Filter	FWHM (mas)	Strehl	Separation (mas)	PA ( $^\circ$ )	$\Delta$ mag
2011.228	$K_S$	50.9 $\pm$ 0.6	0.43 $\pm$ 0.03	212.93 $\pm$ 0.12	122.71 $\pm$ 0.09	2.875 $\pm$ 0.012
2012.171	$Y$	31.8 $\pm$ 1.0	0.05 $\pm$ 0.01	196.9 $\pm$ 0.5	120.75 $\pm$ 0.11	3.13 $\pm$ 0.04
2012.171	$J$	33.9 $\pm$ 1.4	0.12 $\pm$ 0.02	197.8 $\pm$ 0.4	121.2 $\pm$ 0.2	2.96 $\pm$ 0.03
2012.171	$H$	40.2 $\pm$ 1.3	0.22 $\pm$ 0.03	197.9 $\pm$ 0.5	120.9 $\pm$ 0.2	2.95 $\pm$ 0.09
2012.171	$K$	49.8 $\pm$ 0.4	0.45 $\pm$ 0.02	199.5 $\pm$ 0.6	120.54 $\pm$ 0.12	2.85 $\pm$ 0.04

TABLE 3  
PHOTOMETRY OF GJ3629 AB

Property	Primary	Secondary
$R_{\text{USNO-B}}$ (mag)	12.94 <sup>a</sup>	...
$I_{\text{USNO-B}}$ (mag)	10.63 <sup>a</sup>	...
$Y_{\text{MKO}}$ (mag)	9.88 $\pm$ 0.03 <sup>b</sup>	13.01 $\pm$ 0.05
$J_{\text{MKO}}$ (mag)	9.36 $\pm$ 0.02 <sup>c</sup>	12.32 $\pm$ 0.04
$H_{\text{MKO}}$ (mag)	8.82 $\pm$ 0.02 <sup>c</sup>	11.77 $\pm$ 0.09
$K_{\text{MKO}}$ (mag)	8.54 $\pm$ 0.02 <sup>c</sup>	11.39 $\pm$ 0.05
$K_S$ (mag)	8.564 $\pm$ 0.017	11.44 $\pm$ 0.02
$GALEX$ NUV (mag)	19.51 $\pm$ 0.11 <sup>d</sup>	
$GALEX$ FUV (mag)	21.5 $\pm$ 0.4 <sup>d</sup>	
$ROSAT$ flux (erg sec <sup>-1</sup> cm <sup>-2</sup> )	1.0 $\pm$ 0.2 $\times$ 10 <sup>-12e</sup>	
$ROSAT$ HR1	-0.02 $\pm$ 0.16 <sup>e</sup>	
$ROSAT$ HR2	-0.40 $\pm$ 0.20 <sup>e</sup>	

<sup>a</sup> USNO-B photometry from Monet et al. (2003). They estimate the photometric accuracy of the catalog to be 0.3 mag.

<sup>b</sup> Estimated from the  $Y$ - $J$  colors ( $0.52 \pm 0.01$  mag) of M3 dwarfs from Rayner et al. (2009).

<sup>c</sup> Converted to the MKO system from 2MASS (Skrutskie et al. 2006) using the transformation in Leggett et al. (2006).

<sup>d</sup>  $GALEX$  photometry from Morrissey et al. (2007).

<sup>e</sup> From the  $ROSAT$  All-Sky Survey (Voges et al. 1999). The relation from Fleming et al. (1995) was used to convert count rate to flux.

TABLE 4  
 PROPERTIES OF GJ 3629 AB

Property	Primary	Secondary
Age (Myr)	25–300 <sup>a</sup>	
$d_{est}$ (pc)	$22 \pm 3$	
Proj. Sep. (AU)	$4.4 \pm 0.6$	
$\mu_\alpha \cos \delta$ (mas/yr)	$-192.0 \pm 1.0^b$	
$\mu_\delta$ (mas/yr)	$-48.0 \pm 6.0^b$	
$RV$ (km/s)	$13.0 \pm 0.3^c$	
$U$ (km/s)	$-22 \pm 2$	
$V$ (km/s)	$-10.9 \pm 1.6$	
$W$ (km/s)	$3.1 \pm 1.2$	
$X$ (pc)	$-9.9 \pm 1.4$	
$Y$ (pc)	$-1.03 \pm 0.14$	
$Z$ (pc)	$20 \pm 3$	
$\log(L_X/L_{\text{Bol}})$	$-2.90 \pm 0.1$	
$\log(L_{\text{Bol}}/L_\odot)$	$-1.90 \pm 0.13$	$-3.23 \pm 0.14$
Spectral Type	$M3.0 \pm 0.5^a$	$M7 \pm 2^d$
Mass	$0.25 \pm 0.5 M_\odot$	$46 \pm 16 M_{\text{Jup}}$
$P_{\text{Rot}}$ (days)	$3.78^e$	...

NOTE. —  $UVWXYZ$  values are based on the photometric distance estimate.  $U$  and  $X$  are positive toward the Galactic center,  $V$  and  $Y$  are positive toward the direction of galactic rotation, and  $W$  and  $Z$  are positive toward the North Galactic Pole.

<sup>a</sup> Shkolnik et al. (2009).

<sup>b</sup> From the NOMAD catalog (Zacharias et al. 2005).

<sup>c</sup> Shkolnik et al. (2012, submitted).

<sup>d</sup> Estimated from  $YJHK$  colors.

<sup>e</sup> From the HATNet survey (Hartman et al. 2011.)